Distributed control of islanded DC microgrids with solar as grid-forming units

Marco Guerreiro, Pedro dos Santos, Pattarachai Chevathamanon, and Steven Liu
Chair of Control Systems
University of Kaiserslautern-Landau
Kaiserslautern, Germany
marco.guerreiro@rptu.de

***Abstract*—This paper proposes the operation of an islanded microgrid where solar panels are used as grid-forming units. In this way, when conditions are favorable, the microgrid can be entirely operated from solar panels. A battery bank is used to back up generation from the solar panels and share or take over the grid-forming task when necessary. A distributed control approach is used to coordinate the units. Simulation results are shown to support the proposed operation.**

***Index Terms*—dc microgrid, distributed control, grid-forming**

I. Introduction

Microgrids will have an essential role in the power grid of the future, since they provide a way to handle distributed generation and to increase power quality and reliability – all of which are key features of the next generation power grid [1]. To date, the majority of microgrids that were built for research and commercial purposes are AC microgrids, mainly because the current power grid is also AC. However, advances in DC/DC conversion and the fact that most renewable sources, energy storage systems and loads are DC in nature, have contributed for the increasing interest in DC microgrids [2]. DC microgrids can potentially decrease power losses by avoiding AC/DC conversion stages, and can also avoid some of the control issues of AC systems, such as problems with reactive power flow and frequency stability [3].

A microgrid is kept stable by units that stabilize the bus voltage by balancing load and generation [4]. This voltage control varies depending on how the microgrid operates and whether it is connected to an external grid. In grid-connected microgrids, voltage at a common point is usually regulated by the external grid, and units inside the microgrid adjust their voltages with respect to this point in order to exchange power. In islanded microgrids, voltage must be regulated by units inside it. The units responsible for regulating voltage are denoted as grid-forming units.

Typically, grid-forming are units that are dispatchable, i.e. their output power can be adjusted. Examples of such units are generators, energy storage systems and grid-connected converters. Renewable energy sources are usually not employed as grid-forming units because their output power is influenced by external conditions, such as the weather. These units are mostly operated with some maximum power-point tracking strategy, and are denoted as grid-following units.

If renewable resources are always operated in grid-following mode, a grid-forming unit still needs to be active to form and stabilize the bus voltage, even if there is enough power from the renewables to supply the microgrid. Using batteries, generators or grid-connected converters in this case can be inefficient or even have detrimental effects on these units; for example, a generator or a grid-connected converter would be running at low-load conditions and the battery would be constantly charging and discharging. Thus, it can be beneficial if renewable resources could also be also used as grid-forming units, a topic being investigated in many recent studies [5]–[7].

The main contribution of this paper is the proposal of a distributed operation of an islanded microgrid, where solar panels are primarily responsible for stabilizing and forming the grid. This approach allows the microgrid to operate mainly from its solar resources, without requiring a dispatchable unit to form the grid. To handle short- and medium-time variations in solar power, a battery bank is used to back up generation when needed. The battery bank operates in grid-following mode, supporting generation, or operates in grid-forming mode, where it shares or takes over the grid-forming task. Moreover, a supercapacitor bank is used to provide additional power reserve for the grid to handle power transients and to handle transitions between grid-forming units. The units are coordinated through a distributed control scheme, where neighboring units exchange information to control the microgrid. The rest of this paper is organized as follows. Section II presents the case study and assumptions. The proposed operation and distributed controllers are discussed in Section III. Section IV shows simulation results for different operating conditions, and Section V concludes this paper.

II. Case Study and Assumptions

A diagram of the microgrid considered in this study is shown in Fig. 1, which is based on a lab-scale prototype being built. The microgrid has a nominal voltage of 750 V and consists of photovoltaic (PV) units (one rated at 1.2 kWp and two rated at 0.6 kWp), one supercapacitor bank (500 F, rated at 1.2 kW), one battery bank (rated at 1.2 kW), one generator/grid-connected converter (rated at 1.2 kW) and constant power loads (CPLs). The transmission lines are shown in per unit (p.u.), with resistance and inductance of 8.5 Ω and 500 μH p.u., respectively. These are approximate

 DOI 10.1109/eGrid58358.2023.10380844

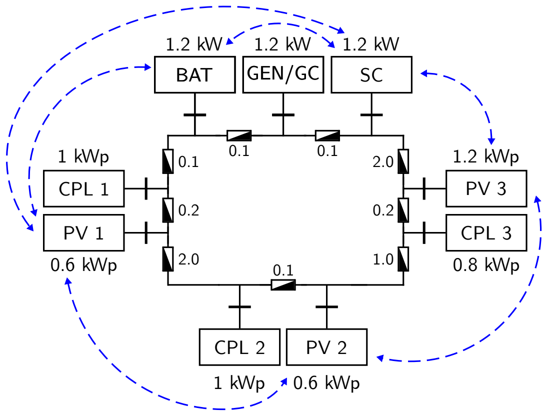

Fig. 1: Diagram of the microgrid under study, including the assumed communication links (dashed blue lines).

per kilometer values for a 2.5 mm^2 cable. Except for the CPLs, the units are assumed to be able to communicate with each other through bidirectional communication links, at a rate of 50 Hz, with a delay of one sample. These links are assumed to be between neighboring units, and are indicated by dashed blue lines in Fig. 1.

All units are assumed to be connected to the microgrid through controlled DC/DC converters. Each converter and its inner control loop is modeled as a voltage or current source, with first order dynamics and limited bandwidth. The supercapacitor unit consists of a supercapacitor and a voltage-controlled converter. This unit is modeled as a voltage source with a state-of-energy (SoE). The SoE indicates the charge stored in the supercapacitor, and is modeled by relating the supercapacitor's total energy to the output power of its DC/DC converter. The solar panel unit consists of a voltage-controlled converter with a maximum power that is given by a maximum power point estimation algorithm. This unit is modeled as a voltage source. The battery bank unit consists of a voltage-controlled converter and is modeled as a voltage source. The battery's state-of-charge (SoC) is not modeled because energy management is not considered in this paper, and because the time scales evaluated are relatively small, it can be assumed that the battery's SoC does not change significantly. Moreover, because the focus is the coordination between the solar panels, supercapacitor and battery bank, the generator/grid-connected is considered to be disconnected at all times.

III. Proposed Operation and Controllers

This section proposes the operation of a microgrid, such that the PV units are mainly responsible for the grid-forming task. The role of the PV, battery, and supercapacitor units are discussed, together with their controllers.

Assuming favorable conditions, a microgrid can be operated entirely from its solar resources, and no additional units need to be connected to the microgrid. In this case, at least one of the PV unit has to take over the grid-forming task. The grid-forming unit stabilizes the bus voltage by matching generation and demand, a process that requires the unit to have some power reserve to be able to suddenly increase or decrease its output power. Because solar panels have a variable maximum power output that depends on weather conditions, a single PV unit may not present enough power reserve to handle transients demanded by the microgrid. However, the power reserve can be increased if all PV units share the grid-forming burden. In this study, all PV units are operated to work in grid-forming mode only, and they share the total microgrid load proportionally to their maximum available power.

Depending on weather and load conditions, the PV units may not have enough power to supply all demand, and voltage stability will be compromised. Moreover, during night time, there will be no output from the solar panels. In such cases, back up generation is required to supply the grid, either by injecting power to support the grid, by sharing the grid-forming burden or by assuming the grid-forming task completely. This paper assumes a microgrid with a battery bank as backup generation, which is operated in grid-following or in grid-forming mode.

In grid-following mode, the battery injects current in the grid to reduce the loading of the PV units, thus giving these units a power reserve. The amount of current to be injected by the battery can be regulated by the desired power reserve. If, however, the current required to regulate this loading is too large, it is an indication that the PV units do not have enough power, and this information can be used to change the battery to grid-forming mode. In grid-forming mode, the battery shares the total microgrid load with the other PV units, proportionally to its power rating. The battery can transition back to grid-following mode when its output current gets below a certain threshold, indicating that there is enough power from the other units to supply the grid.

Because there will be transitions between units performing the grid-forming task, it might happen that there will be short time instants where the grid has no grid-forming unit. This can introduce large deviations on the bus voltage, or even lead to instability. This problem can be avoided if there is a grid-forming unit that is always connected to the microgrid. This unit, however, does not need to share the grid-forming burden in steady-state, but only during transients. One candidate for such task is a supercapacitor unit. Supercapacitors are devices with high power/low energy density, meaning that they are able to supply large peaks of power, but for limited amounts of time. Moreover, the life cycle of supercapacitors is much larger than that of batteries. These features make them well suited for balancing generation and demand in a microgrid for short periods of time, while other units are still picking up the load [4]. Thus, the supercapacitor unit is operated as grid-forming mode, but it does not supply any load during steady state, i.e. it does not share the load with the other grid-forming units. The supercapacitor units is operated such that it supplies the load only during transients.

To summarize, the operation of microgrid is as follows. The PV units always work in grid-forming mode, and share the total load proportionally to their maximum available power. The supercapacitor unit always work as grid-forming mode,

 DOI 10.1109/eGrid58358.2023.10380844

but only supplies the grid during transients, not actively sharing the load with the other units. The battery unit can operate in grid-following or grid-forming mode, depending on the loading of the PV units.

The grid-forming units have the task to stabilize the voltage. However, in a DC microgrid, the voltage cannot be controlled to the same reference everywhere, otherwise there will be no power transfer between the units. One alternative is to regulate the average voltage between the grid-forming units. Thus, the average voltage between the units sharing the grid-forming task is regulated to a reference value.

Next, distributed average voltage control and load sharing is discussed, as well as the controllers for each unit.

A. Average voltage control and load sharing

Units participating in average voltage control have a proportional-integral (PI) controller that works to drive the average voltage across the microgrid to a reference value. These local controllers need to estimate the average voltage between the grid-forming units, and this is achieved through a dynamic consensus algorithm. The estimated average voltage $v_{\mathrm{avg},i}$ of the i-th unit is given by [8]

$$v_{\mathrm{avg},i}(t) = v_i(t) + \int_0^t \sum_{j\in N_j} \alpha_{i,j}\big(v_{\mathrm{avg},j}(\tau) - v_{\mathrm{avg},i}(\tau)\big)\mathrm{d}\tau, \quad (1)$$

where v_i is the local voltage measurement of the i-th unit, and $\alpha_{i,j}$ is a coefficient that is one when there is a communication link between units i and j, and zero otherwise. Under the conditions that the graph formed by the communication links between the units is undirected and connected, it can be shown that the average voltage $v_{\mathrm{avg},i}$ computed by the i-th unit converges to the average between all local voltage measurements [9].

Units sharing the load have another PI controller that works to drive the difference of the p.u. current between them to zero. The current error signal $\Delta i_{\mathrm{pu},i}$ of the i-th unit is obtained through [8]:

$$\Delta i_{\mathrm{pu},i}(t) = \sum_{j\in N_j} \beta_{i,j}\big(i_{\mathrm{pu},j}(t) - i_{\mathrm{pu},i}(t)\big), \quad (2)$$

where $\beta_{i,j}$ is one when there is a communication link between units i and j, and zero otherwise.

The average voltage and current sharing controllers are shown in Fig. 2. The average voltage controller is shown in Fig. 2a, and processes the difference between the microgrid reference voltage v^* and the average voltage across the microgrid, as estimated by the i-th unit using (1). The result is the correction term $\delta v_{\mathrm{avc},i}$. Similarly, the current sharing controller, shown in Fig. 2b, processes the current difference given by (2), and produces the correction term $\delta v_{\mathrm{cs},i}$.

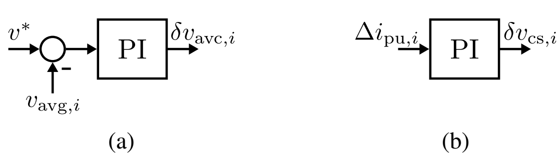

Fig. 2: (a) Average voltage and (b) current sharing controllers.

B. PV unit controller

The reference voltage signal $v_{\mathrm{pv},k}$ of the k-th PV unit is

$$v_{\mathrm{pv},k} = \delta v_{\mathrm{dr,pv},k} + \delta v_{\mathrm{avc,pv},k} + \delta v_{\mathrm{cs,pv},k}, \quad (3)$$

where $\delta v_{\mathrm{dr,pv},k}$ is a droop term given by

$$\delta v_{\mathrm{dr,pv},k} = v^* - r_{\mathrm{d},k} i_k, \quad (4)$$

where v^* is the microgrid reference voltage, $r_{\mathrm{d},k}$ is the droop coefficient and i_k is the output current of the k-th unit. The terms $\delta v_{\mathrm{avc,pv},k}$ and $\delta v_{\mathrm{cs,pv},k}$ are generated by the average voltage and load sharing controllers, shown in Fig. 2.

C. Supercapacitor unit controller

The reference voltage v_{sc} of the supercapacitor unit is

$$v_{\mathrm{sc}} = \delta v_{\mathrm{dr,sc}} + \delta v_{\mathrm{avc,sc}} + \delta v_{\mathrm{SoE}}, \quad (5)$$

where $\delta v_{\mathrm{dr,sc}}$ is a droop term, $\delta v_{\mathrm{avc,sc},k}$ is the average voltage control correction term and v_{SoE} is a signal generated by the SoE controller of the supercapacitor unit. The droop term follows the structure given by (4), while the average control correction term is generated by the controllers shown in Fig. 2.

The SoE correction signal is given by the controller shown in Fig. 3. The SoE is estimated by integrating the output power of the unit (p_{sc}) considering an initial SoE (SoE_0). The difference between the reference and estimated SoE values is processed by a PI controller, which generates the δv_{SoE} correction term. By regulating the SoE to a constant value, the supercapacitor unit does not supply any current at steady-state. The SoE controller is designed to be slower than the average voltage controller, such that the supercapacitor unit shares the grid-forming task during transients, but does not supply any load at steady-state. Moreover, the reference SoE is chosen as 50%. This gives the unit a margin so that it can supply power when a load is connected to the grid, and also absorb excess power when a load is disconnected.

D. Battery unit controller

Fig. 4 shows the battery controllers. As shown in Fig. 4a, the reference signal v_{bat} for the battery unit is given by

$$v_{\mathrm{bat}} = \delta v_{\mathrm{dr,b}} + (1-\gamma)\delta v_{\mathrm{cc,b}} + \gamma(\delta v_{\mathrm{avc,b}} + \delta v_{\mathrm{cs,b}}), \quad (6)$$

where $\delta v_{\mathrm{dr,b}}$ is a droop term, $\delta v_{\mathrm{cc,b}}$ is the command from the battery's current controller, $\delta v_{\mathrm{avc,b}}$ and $\delta v_{\mathrm{cs,b}}$ are commands from the average voltage and current sharing controllers, and

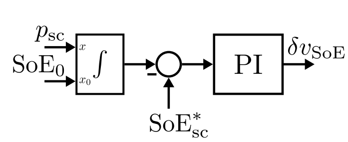

Fig. 3: SoE controller of the supercapacitor unit.

 DOI 10.1109/eGrid58358.2023.10380844

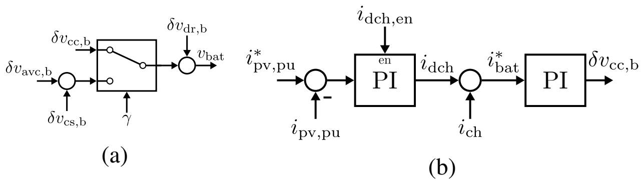

Fig. 4: (a) Battery and (b) battery current controllers.

γ is a binary variable that depends on the operation mode of the battery.

When in grid-following mode ($\gamma = 0$), the battery is operated as a current source, regulated by the current controller shown in Fig. 4b. The battery current i^*_{bat} is determined by the superposition of a charging (i_{ch}) and discharging (i_{dch}) current. The charging current comes from an external energy management system that would regulate the SoC of the battery. The discharging current comes from a controller that regulates the loading of the PV units. This controller has an enable signal, $i_{\text{dch,en}}$, that is activated when overloading of the PV units is detected. In this case, the controller regulates the loading of the PV units to a reference value $i^*_{\text{pv,pu}}$. If the discharge current becomes negative, this means that to control the loading of the PV units, the battery has to sink current. This indicates that the PV units have enough power to supply the grid without overloading, and the discharge current controller can be disabled. If, on the other hand, the discharge current increases above a certain threshold, this indicates that there may not be enough power from the other units to supply the grid, and voltage regulation could be compromised. In this case, the battery switches to grid-forming mode.

In grid-forming mode ($\gamma = 1$), the battery participates in average voltage control and current sharing. When the current supplied by the battery is below a certain threshold, the battery can switch back to grid-following mode, as there is enough power from the other sources to support voltage control.

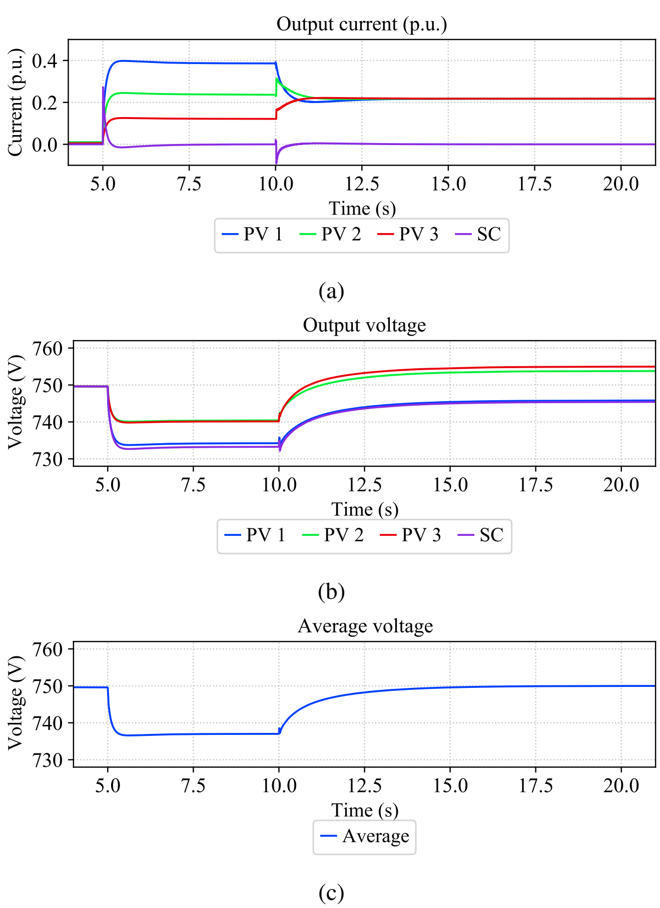

Fig. 5: (a) Output current, (b) output voltage and (c) average voltage of active units with droop control only, and with average voltage control and load sharing.

IV. Simulation results

This section shows simulation results obtained with the proposed controllers. The microgrid shown in Fig. 1 was simulated using the PLECS software. The battery current controller was set to activate when the p.u. current of the PV units exceeded 0.825. The battery was set to change to grid-forming mode when its own p.u. current exceeded a value of 0.5. A dead-band of 0.05 was added to this value, in order to prevent switching between grid-forming and grid-following modes when the p.u. current of the battery is around 0.5.

A. Average voltage control and current sharing

Fig. 5 shows current sharing and average voltage control. Initially, only droop control is active in all units, and there is no load connected to the grid. At 5 s, CPL 1 is connected to the grid and consumes 0.5 kW. Fig. 5a shows how the supercapacitor is quickly discharged to supply the load and then charges slowly to regulate its SoE. Moreover, from Figs. 5b and 5c, it is possible to see that the voltage drops when the load is connected, due to droop control. At 10 s, current sharing and average voltage control are enabled, and it is possible to note that the solar panels share their p.u. current, and all voltages are adjusted such that the average voltage is driven to the reference value.

B. Battery in grid-following mode

Fig. 6 shows the battery operating in grid-following mode. Initially, CPL 1 is consuming 1 kW. At this moment, the p.u. current of the solar panels are around 0.4, and the battery does not inject any current into the grid. At 20 s, CPL 2 starts consuming 1 kW. Since the p.u. current of the PV units gets above 0.8 p.u., the battery starts injecting current into the grid in order to regulate the PV units' p.u. current to 0.8. At 30 s, CPL 2 is disconnected, and the battery stops discharging since the p.u. current of the PV units is below 0.8.

Fig. 7 shows a case where the battery is charging, and then its charging current is adjusted to not overload the PV units. Initially, CPL 1 and CPL 2 are consuming 0.4 kW each. At 10 s, the battery starts charging. At this point, the solar panels have enough power to supply the loads and charge the battery. At 15 s, CPL 3 starts consuming 0.65 kW. At this point, the

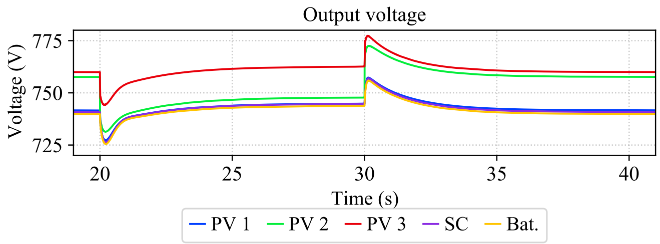

(a)

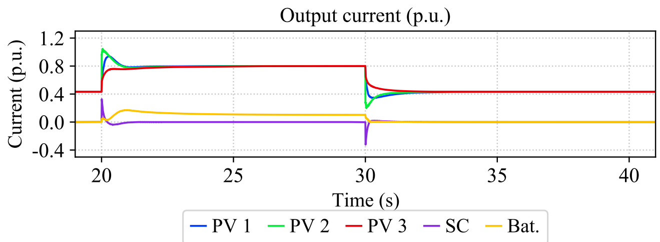

(b)

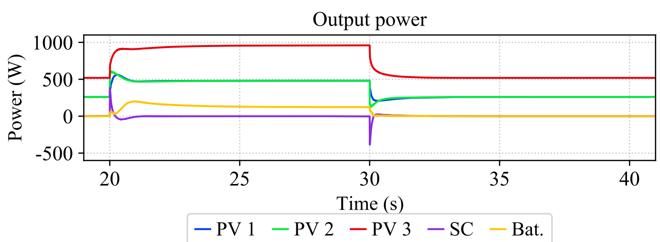

(c)

Fig. 6: (a) Output voltage, (b) output current and (c) output power of active units when the battery operates in grid-following mode.

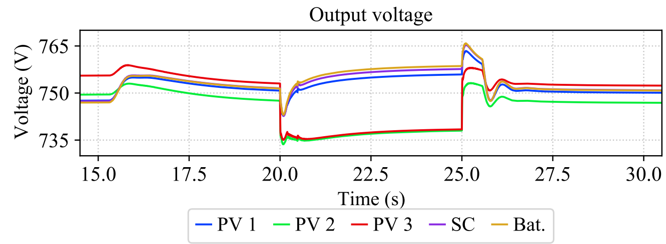

(a)

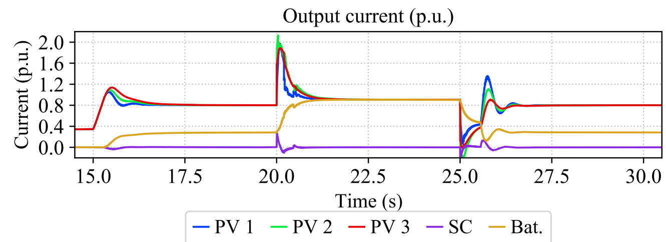

(b)

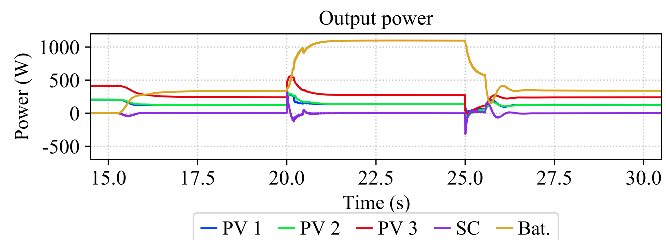

(c)

Fig. 8: (a) Output voltage, (b) output current and (c) output power of active units when the battery switches between grid-following and grid-forming modes.

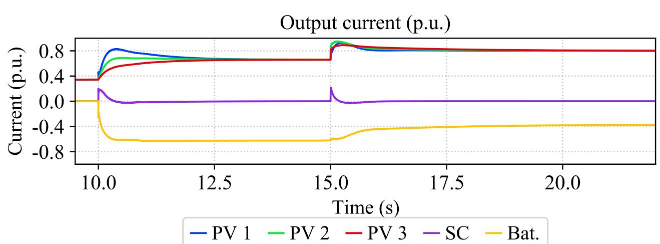

Fig. 7: Output current of the units when the battery is charging.

p.u. current of the PV units goes above 0.8. Then, the discharge current controller regulates the battery's current in order to regulate the p.u. current of the PV units to 0.8. However, the battery still charges, although at a lower current.

C. Battery in grid-forming mode

Fig. 8 shows a case where the battery switches between grid-supporting and grid-forming modes. Initially, the solar panels are supplying CPLs 1 and 2, each consuming 0.4 kW. At 15 s, the solar panels lose 75% of their generation. Since their p.u. current exceeds 0.8, the battery starts injecting current to stabilize the panels' loading at 0.8. At this moment, the battery still operates in grid-following mode. At 20 s, CPL 3 starts consuming 0.8 kW. This load causes the output current of the battery to increase above 0.5 p.u., which triggers the grid-forming mode. At this moment, the battery starts participating in average voltage control and load sharing. At 25 s, CPL 3 is disconnected, and the battery changes back to grid-following mode, since its current is below the 0.5 p.u. threshold.

D. Operation under disconnection of PV units

Fig. 9 shows a case where one of the PV units is disconnected from the microgrid. Initially, all three PV units are connected, and supplying CPLs 1 and 2, each consuming 0.4 kW. At 15 s, PV unit 3 is disconnected from the grid, and the remaining PV units share their p.u. current and regulate the average voltage. At 25 s, PV 3 is connected back, and load sharing and voltage control is achieved by all three units again.

Fig. 10 shows a case where all the PV units are disconnected from the grid. Initially, all PV units are connected, and supply CPLs 1 and 2, each consuming 0.2 kW. At 20 s, the solar panels are disconnected, and the battery enters grid-forming

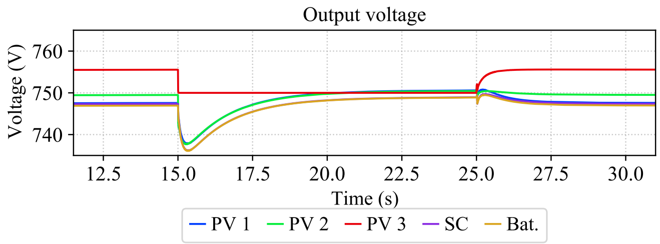

(a)

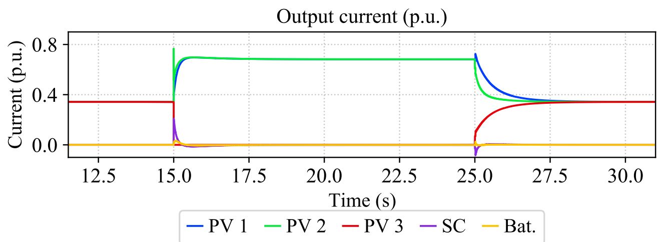

(b)

Fig. 9: (a) Output voltage and (b) output current of active units, when PV unit 3 is disconnected from the microgrid.

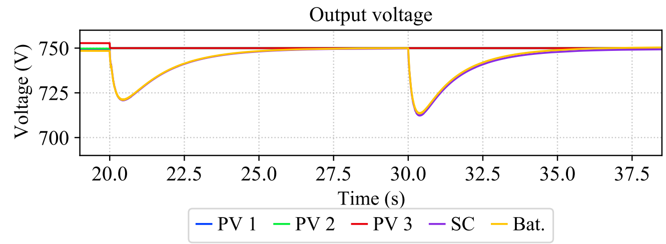

(a)

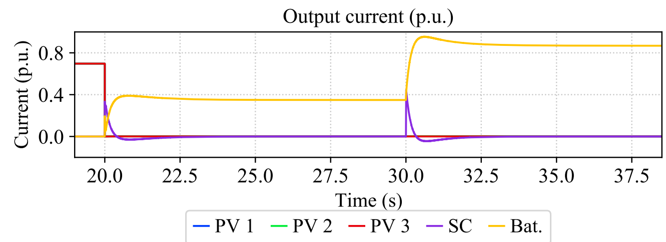

(b)

Fig. 10: (a) Output voltages and (b) currents, when the PV units are disconnected.

mode and, together with the supercapacitor unit, regulates the average voltage across the microgrid. At 30 s, CPL 3 starts consuming 0.6 kW. As Fig. 10 shows, the battery is able to stabilize the microgrid voltage; however, voltage deviations are larger when the battery and the supercapacitor are the only units forming the grid.

V. Conclusions

This paper discussed a distributed control approach, along with local controllers, that allows a DC microgrid to be operated mainly from solar panels. These units share the grid-forming task with a supercapacitor bank, while a battery bank is used to back up generation from the solar panels, and to share or take over the grid-forming task. The approach discussed is able to provide a power margin when the grid is operated through solar panels, an important feature for grid-forming units.

The next expansion of the method presented in this paper is to include the SoC of the battery. In this case, the microgrid needs a generator, or a grid-connected converter, that is able to supply the grid when there is no power from the PV units, and the battery is empty. The coordination between these units takes place at two different levels. At a low level, the battery and generator/grid-connected converter communicate to stabilize the grid voltage. At a higher level, an energy management system is required, in order to regulate the SoC of the battery.

References

[1] A. Hirsch, Y. Parag, and J. Guerrero, "Microgrids: A review of technologies, key drivers, and outstanding issues," *Renew. Sustain. Energy Rev.*, vol. 90, pp. 402–411, 2018.

[2] L. E. Zubieta, "Are microgrids the future of energy? DC microgrids from concept to demonstration to deployment," *IEEE Electrif. Mag.*, vol. 4, no. 2, pp. 37–44, 2016.

[3] V. F. Pires, A. Pires, and A. Cordeiro, "DC microgrids: Benefits, architectures, perspectives and challenges," *Energies*, vol. 16, no. 3, 2023.

[4] I. Serban, "A control strategy for microgrids: Seamless transfer based on a leading inverter with supercapacitor energy storage system," *Applied Energy*, vol. 221, pp. 490–507, 2018.

[5] B. Pawar, E. I. Batzelis, S. Chakrabarti, and B. C. Pal, "Grid-forming control for solar PV systems with power reserves," *IEEE Trans. Sustain. Energy*, vol. 12, no. 4, pp. 1947–1959, 2021.

[6] R. H. Lasseter, Z. Chen, and D. Pattabiraman, "Grid-forming inverters: A critical asset for the power grid," *IEEE J. Emerg. Sel. Topics Power Electron.*, vol. 8, no. 2, pp. 925–935, 2020.

[7] M. E. Elkhatib, W. Du, and R. H. Lasseter, "Evaluation of inverter-based grid frequency support using frequency-watt and grid-forming PV inverters," in *2018 IEEE PESGM*, 2018, pp. 1–5.

[8] V. Nasirian, S. Moayedi, A. Davoudi, and F. L. Lewis, "Distributed cooperative control of DC microgrids," *IEEE Trans. Power Electron.*, vol. 30, no. 4, pp. 2288–2303, 2015.

[9] D. P. Spanos, R. Reza Olfati-Saber, and R. M. Murray, "Dynamic consensus for mobile networks," in *Proc. 16th IFAC World Congr*, 2005, pp. 1–6.